Shape anisotropy of a single random-walk polymer

Charbel Haber*, Sami Alom Ruiz*, and Denis Wirtz*†‡

*Department of Chemical Engineering and †Department of Materials Science and Engineering, The Johns Hopkins University, 3400 North Charles Street, Baltimore, MD 21218

Communicated by Robert H. Austin, Princeton University, Princeton, NJ, July 10, 2000 (received for review March 13, 2000)

Random walks have been used to describe a wide variety of systems ranging from cell colonies to polymers. Sixty-five years ago, Kuhn [Kuhn, W. (1934) *Kolloid-Z.* 68, 2–11] made the prediction, backed later by computer simulations, that the overall shape of a random-walk polymer is aspherical, yet no experimental work has directly tested Kuhn's general idea and subsequent computer simulations. By using fluorescence microscopy, we monitored the conformation of individual, long, random-walk polymers (fluorescently labeled DNA molecules) at equilibrium. We found that a polymer most frequently adopts highly extended, nonfractal structures with a strongly anisotropic shape. The ensemble-average ratio of the lengths of the long and short axes of the best-fit ellipse of the polymer was much larger than unity.

Random walks have been extensively used to describe a multitude of phenomena, ranging from cell migration within connective tissues, to Markov processes in DNA sequences, to time series in the stock market, to diffusion in gas, liquids, and solids (1–5). Sixty-five years ago, Kuhn (6) predicted that the shape of a random-walk polymer is *not* spherically symmetric, i.e., a regular random walk has an overall shape which is anisotropic. The intuitive idea of a spherical shape is based on a flexible polymer (or a random walk) having an isotropic end-to-end vector distribution and on the implicit rotational averaging typically done in polymer theories and experiments (7–10), yet the shape of individual polymers has not been probed directly (5, 9).

The lack of direct conformational information has so far prevented a direct test of Kuhn's prediction (6), which is supported by computer simulations (11–16) and analytical calculations (5). Bulk measurements such as light scattering and rheology (17, 18) are inappropriate to probe the behavior of individual polymers in solution. These bulk experimental methods average the orientation, shape, and dynamics of a large ensemble of molecules simultaneously. Here, by monitoring the conformation, orientation, and dynamics of individual flexible polymers in dilute solutions, we directly measure the *distributions* of conformational parameters. We therefore test Kuhn's central prediction directly.

Materials and Methods

Light microscopy (Nikon) equipped with a ×100, n.a. 1.30, oil-immersion lens was used to monitor the conformation of individual, fluorescently labeled DNA molecules at equilibrium. We used monodisperse Coliphage T2-phage DNA (T2-DNA) molecules (19) suspended at a concentration ≈20 ng/ml (much smaller than the overlap concentration ≈0.13 mg/ml) in Tris·EDTA buffer and an oxygen-scavenging system to reduce photobleaching (20–22). DNA molecules were stained with an intercalating dye (YOYO-1, Molecular Probes), which we verified did not affect the overall shape distribution of DNA. T2-DNA is a highly flexible polymer with a contour length of $L \approx 56$ μm and a persistence length of $l_p \approx 52$ nm. Hence, this polymer is a linear sequence of ≈1,075 ($= L/l_P \gg 1$) statistical segments whose orientations are not correlated.

To measure the shape of flexible polymers in an unconfined geometry and limit long-range hydrodynamic interactions between polymers and chamber walls (unlike Yanagida *et al.*, ref. 22), DNA solutions were slowly introduced into a custom-built, large-gap microscopy chamber (gap size = 300–500 μm ≫ radius of gyration $R_g \approx 1.5$ μm) (21). Individual polymers were monitored at the midplane of the chamber, for which we verified that no hydrodynamic interactions with chamber walls were present. The molecular integrity of DNA was verified to be preserved during microscopy experiments by measuring, after each experiment, DNA molecular weight via gel electrophoresis (23). Because a shear flow can easily stretch and orient flexible polymers (21), it was verified that no convection was present during the measurements by monitoring the longtime displacement of each probed polymer (Fig. 1*C*, which shows no bias in polymer orientation) to ensure that we monitored polymers in the absence of an external flow field. Individual polymers were chosen randomly in different fields of view. For each polymer, the shape and conformational dynamics was measured for an extended period (≈100 s ≫ relaxation time of the polymer $\tau = 1.0 \pm 0.2$ s). The overall shape of the fluorescently labeled polymer was analyzed by enveloping its trace by an ellipse that encompassed all segments of the polymer and computed the lengths of the major and minor axes as well as the orientation of the resulting ellipse (Fig. 1*A* for definitions).§

Results and Discussion

As we expected, we found that a single flexible polymer probed over a sufficiently long period (Fig. 2*C*) or a large ensemble of flexible polymers probed at random (Fig. 1*C*) had an isotropic distribution of orientations. Figs. 1*B* and 2 *A* and *B* illustrate the seemingly random orientation of a single flexible polymer. The distribution function of the instantaneous orientation angle was flat (Fig. 2*C*). The same result holds for individual polymers captured at random. The angular distribution of a large ensemble of polymers was isotropic (Fig. 1*C*).

However, we observed that a single flexible polymer adopts conformations that were much more open and extended than typically presumed in standard models (Fig. 2*A*). Our microscopy experiments showed that flexible polymers adapted extended conformations most frequently (Fig. 2*A*). Fig. 2*A* shows the dynamic conformation of a single DNA molecule as a function of time. This polymer fluctuated ("breathes") rapidly between collapsed and extended configurations (Fig. 2*D*), whereas the overall shape of the polymer rotated rapidly (Fig. 2*B*). Despite the entropic cost of large polymer extensions, we observed, during the course of polymer fluctuations, extensions of up to $2l_{major}/L \approx 25\%$, which corresponds to a shape defor-

Abbreviation: T2-DNA, Coliphage T2-phage DNA.

‡To whom reprint requests should be addressed. E-mail: wirtz@jhunix.hcf.jhu.edu.

§The choice of an ellipse is somewhat arbitrary. However, by exploiting the spatial distribution of the fluorescent intensity of the trace of each polymer that describes the local segment density (such as shown in Fig. 2*A*), we also characterized the shape anisotropy of flexible polymers by using the two specific orthogonal components of the radius of gyration taken along its principal axes of inertia (5, 15). We obtained an ensemble-averaged aspect ratio $\langle r \rangle \approx 2.5$ similar to that obtained by using a best-fit ellipse that encompasses all the segments of the polymer.

The publication costs of this article were defrayed in part by page charge payment. This article must therefore be hereby marked "*advertisement*" in accordance with 18 U.S.C. §1734 solely to indicate this fact.

Article published online before print: *Proc. Natl. Acad. Sci. USA*, 10.1073/pnas.190320097. Article and publication date are at www.pnas.org/cgi/doi/10.1073/pnas.190320097

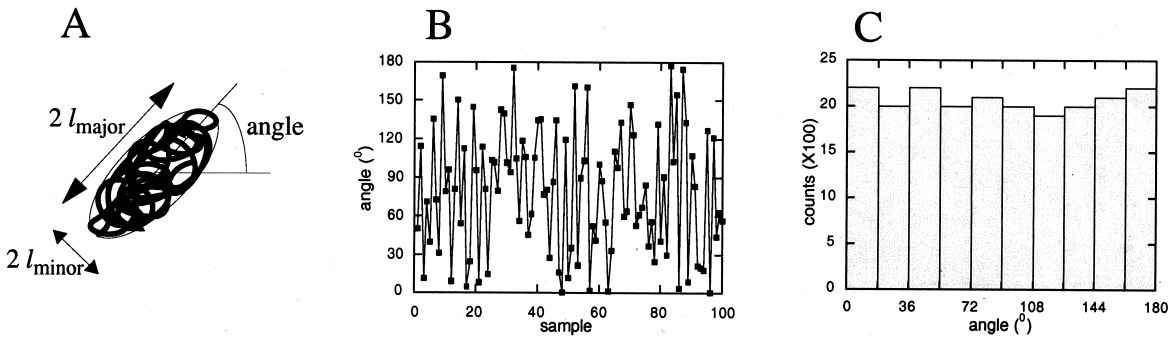

Fig. 1. Definitions and measurements of shape anisotropy and orientation of fluorescently labeled DNA molecules probed via light microscopy (*A*) Nonspherical shape of a random-walk polymer, as predicted by Kuhn (6) and observed in this study. The best-fit ellipse encompasses all segments of the polymer and defines the lengths of the large axis and the minor axis, l_{major} and l_{minor}, respectively, as well as the angle of orientation, θ. (*B*) Sampled values of the orientation of polymers chosen at random in different fields of view and different samples. (*C*) Distribution of the angle of orientation of a large ensemble of flexible polymers.

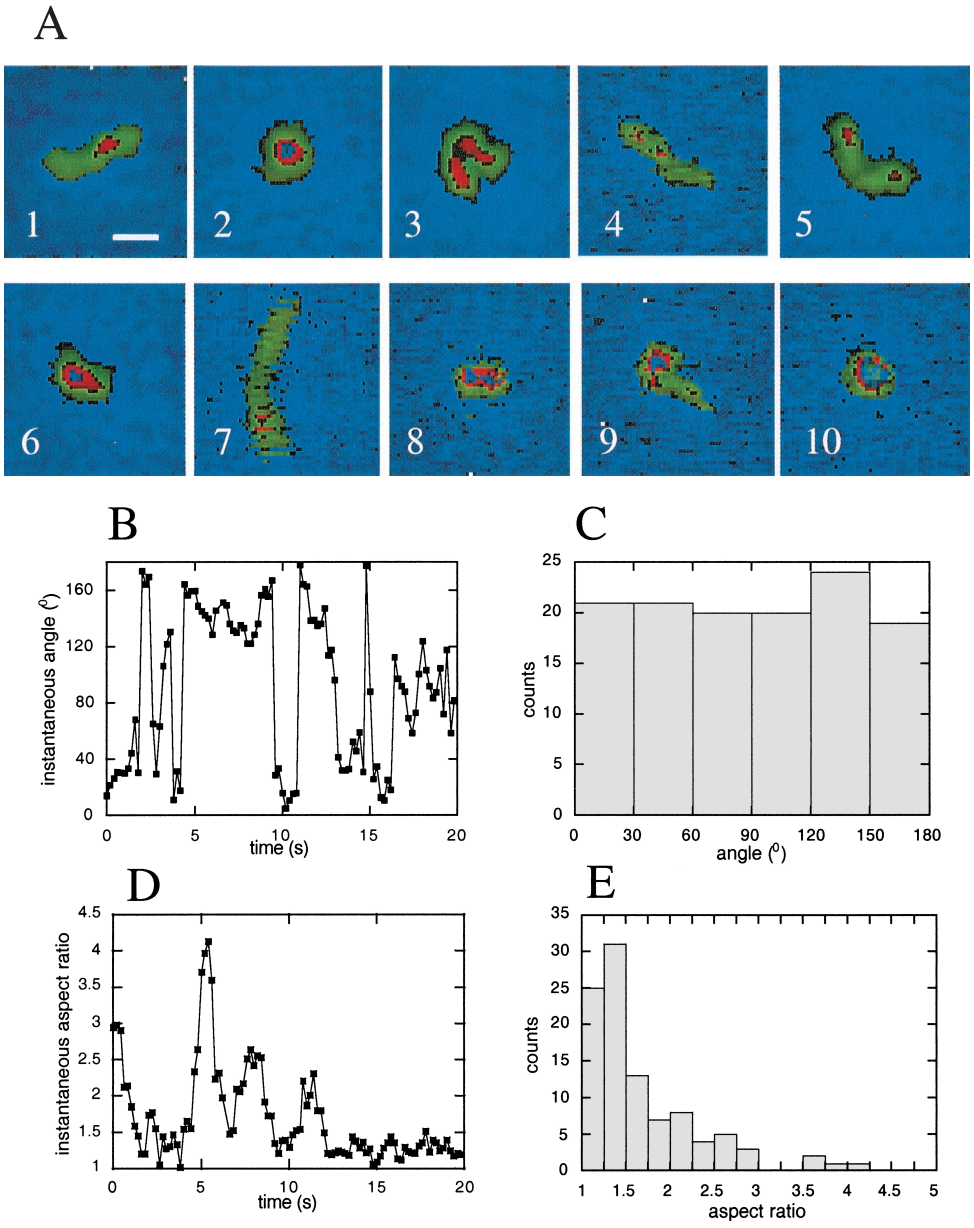

Fig. 2. Fluctuations and associated time-based distribution of shape per orientation of a single polymer. (*A*) Typical evolution of the conformation of a single DNA polymer in Tris-EDTA buffer; 2 s are between each frame. (*B*) Instantaneous angle of orientation for the fluctuating polymer shown in *A*. (*C*) Associated distribution of the angle of orientation. (*D*) Instantaneous aspect ratio of the ellipse, $r = l_{major}/l_{minor}$, for the polymer shown in *A*. (*E*) Associated distribution of the aspect ratio. (Calibration bar represents 1 μm.)

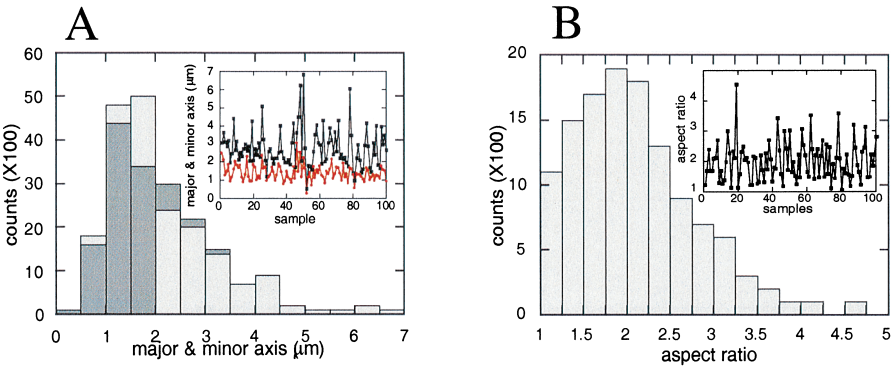

Fig. 3. Ensemble-based distribution of shape anisotropy of individual polymers. (*A*) Distribution of the lengths of the major (dark shading) and minor (light shading) axes for a large ensemble of flexible polymers. (*Inset*) Randomly sampled lengths of major (upper curve) and minor (lower curve) axes. (*B*) Distribution of the aspect ratio for a large ensemble of flexible polymers; $<r> = <l_{major}/l_{minor}> = 2.2 \pm 0.75$. (*Inset*) Randomly sampled aspect ratio.

mation of about $(l_{major} - R_g)/R_g \approx 370\%$ (data taken from Fig. 3*A*).

We quantified the overall shape of free individual, flexible polymers. We replaced each image of a fluctuating polymer by a best-fit ellipse (Fig. 1*A*) and measured the lengths of the long and minor axes as a function of time for a single polymer or an ensemble of randomly selected polymers. The lengths of the long and minor axes fluctuated seemingly randomly and not synchronously (Fig. 3*A*). As a result, we found that the aspect ratio (ratio of major axis over minor axis) varied widely, yet was larger than unity 95% of the time. The time-averaged aspect ratio (Fig. 2*E*) and ensemble-averaged aspect ratio (Fig. 3*B*) were found to be equal to 2.20 ± 0.7 (means ± SD), which was an underestimate of the true three-dimensional aspect ratio of the polymer. To measure polymer shape anisotropy in three dimensions, we suspended fluorescently labeled T2-DNA molecules in high-viscosity, sucrose-containing buffer and conducted fast *z*-scans by using a confocal microscope (Noran Instruments, Middleton, WI). We observed that a flexible polymer was best described by a prolate ellipsoid and found ensemble-average aspect ratios ≈4.1:2.3:1 along the moments of the radius of gyration.

We observed extremely rapid rates at which the aspect ratio of a flexible polymer and orientation changed with time (Fig. 2 *B* and *D*). The rate of change of the aspect ratio, $<r>^{-1}\Delta r/\Delta t$, where $r = l_{major}/l_{minor}$ and $<r> = 2.2$, ranged between 0 and ≈3.2 s^{-1} (Fig. 4*A*) in Tris·EDTA buffer and the rate at which a polymer rotated by more than 90°, $2\pi^{-1}\Delta\theta/\Delta t$, ranged between 0 and ≈5 s^{-1} (Fig. 4*B*). Hence, the time scale of reorientation and time scale of shape change were shorter than the relaxation time associated with the translational diffusion of the polymer, $\tau = 1.0 \pm 0.2$ s. Of note, the rates of reorientation and polymer remodeling evolved seemingly randomly over time (insets in Fig. 4 *A* and *B*).

Is this large shape anisotropy simply caused by the finite flexibility of T2-DNA? The bending rigidity of DNA molecules has been studied extensively (17–19) and is described by the persistence length (24, 25). The persistence length corresponds to the curvilinear length required to travel along the polymer to reach near-complete orientation decorrelation. The persistence length of DNA has been measured by using various approaches including dynamic light scattering and force-measuring laser tweezers, and depends mostly on ionic nature and strength of the solvent (24, 25). In the present conditions, the persistence length of T2-DNA, l_p, is orders of magnitude shorter than its contour length, L ($L = 56$ μm vs. $l_P = 52$ nm). Hence, T2-DNA is a highly flexible molecule. Furthermore, DNA molecules follow stretch-force curves predicted for flexible polymers (24). To investigate the dependence of the shape anisotropy on the ratio L/l_p that describes the flexibility of linear polymers, we used two types of DNA molecules of lengths 56 μm (T2-DNA) and 22 μm (λ-phage DNA) (23) and varied the ionic strength of the buffer from 0 to 200 mM NaCl, which decreased l_p from 120 to 48 nm (24, 25). We found similar distributions for the angle of orientation and slightly increasing values of the ensemble- and time-averaged aspect ratio for increasing values of L/l_p ($1{,}170 \geq L/l_P \geq 170$; data not shown).

Is the polymer shape anisotropy caused by intramolecular, self-avoiding interactions? Aronovitz and Nelson (26) showed

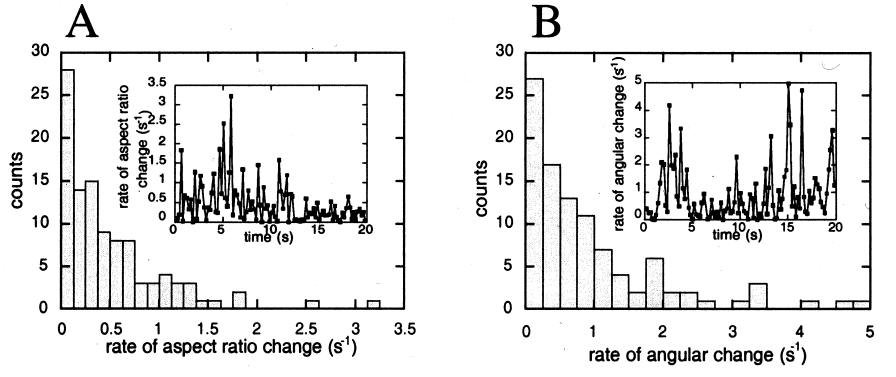

Fig. 4. Instantaneous rates of polymer remodeling and reorientation. (*A*) Distribution of the instantaneous rate of change of the aspect ratio, $<r>^{-1}\Delta r/\Delta t$ where $r = l_{major}/l_{minor}$, $<r> = 2.2$, and $\Delta t = 0.2$ s. (*Inset*) Typical evolution of the instantaneous rate change of the aspect ratio. (*B*) Distribution of the instantaneous rate of change of polymer reorientation, $2\pi^{-1}\Delta\theta/\Delta t$. (*Inset*) Typical evolution of the instantaneous rate of change of polymer reorientation.

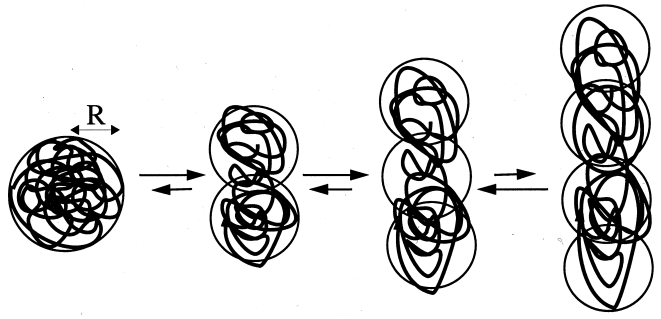

Fig. 5. Proposed model of shape anisotropy of a polymer at equilibrium based on the results of this paper and ref. 9. One can decompose a spherically symmetric polymer of given radius *R* into two (possibly overlapping) spheres of equal radius $< R$ and "squeeze" all of the segments of the polymer into these two spheres. The loss in entropy caused by the longitudinal stretching and lateral compression of the polymer would be more than compensated by the appearance of new degrees of freedom, i.e., the relative separation between the two spheres and their relative orientation. This decomposition can be extended to three spheres, etc., until polymer deformation becomes entropically too unfavorable compared with the entropic gain caused by additional degrees of freedom.

theoretically that the asymmetry of a self-avoiding random walk was only slightly more pronounced than that predicted by Kuhn (6) for a regular random walk. Moreover, self-avoidance (steric) interactions among segments of a DNA molecule are expected to become important only when the DNA contour length becomes larger than $8\ l_p^3/D^2 \approx 62\ \mu$m, where $D \approx 4$ nm is the hard-core diameter of DNA (27). Hence, T2-DNA molecules used in this study ($L = 56\ \mu$m $< 62\ \mu$m) adopted a random-walk conformation, i.e., intramolecular interactions were negligible. Therefore, the large-shape anisotropy of a flexible polymer was caused neither by intramolecular interactions nor by the nonzero rigidity of the DNA molecules used in this study. Following Kuhn (6), we conclude that the predominance of extended structures of nonspherical symmetry is a general feature of flexible polymers in solution and is caused by their random-walk nature.

The origin of this shape anisotropy could be understood as follows (9). One can decompose a spherically symmetric polymer of given radius *R* into two (possibly overlapping) spheres of equal radius $< R$ and "squeeze" all of the segments of the polymer into these two spheres (Fig. 5 and ref. 9). The loss in entropy caused by the longitudinal stretching and lateral compression of the polymer would be more than compensated by the appearance of new degrees of freedom, the relative separation between the two spheres, and their relative orientation. This decomposition can be extended to three spheres, etc., until polymer deformation becomes too unfavorable compared with the entropic gain caused by additional degrees of freedom. This decomposition defines an intermediate extension and associated shape anisotropy (9).

Our results constitute direct experimental support for Kuhn's prediction on the shape of random walks and may help refine current theories of polymer dynamics. For instance, our observations explain the easier-than-expected stretching of flexible polymers by a shear flow (21), because polymers that display large extensions can couple to a flow much more readily than polymers with a globular conformation.

We thank R. D. Kamien, M. Li, and M. Ferro for insightful discussions and M. Delannoy for confocal microscopy. This work was supported by the National Aeronautics and Space Administration (NAG81377), the National Science Foundation (DMR9623972), and Merck.

1. Pearson, K. (1905) *Nature (London)* **27,** 239–242.
2. Einstein, A. (1906) *Ann. Phys.* **19,** 2–7.
3. Sharpe, W. S. (1970) *Portfolio Theory and Capital Markets* (McGraw–Hill, New York).
4. Berg, H. C. (1993) *Random Walks in Biology* (Princeton Univ. Press, Princeton), pp. 2–100.
5. Rudnick, J. & Gaspari, G. (1987) *Science* **237,** 384–389.
6. Kuhn, W. (1934) *Kolloid-Z.* **68,** 2–11.
7. de Gennes, P.-G. (1991) *Scaling Concepts in Polymer Physics* (Cornell Univ. Press, Ithaca, NY), pp. 13–32.
8. Flory, P. J. (1953) *Principles of Polymer Chemistry* (Cornell Univ. Press, Ithaca, NY).
9. Triantafillou, M. & Kamien, R. D. (1999) *Phys. Rev. E Stat. Phys. Plasmas Fluids Relat. Interdiscip. Top.* **59,** 5621–5624.
10. Doi, M. & Edwards, S. F. (1989) *Theory of Polymer Dynamics* (Clarendon, Oxford), pp. 2–45.
11. Gobush, W., Solc, K. & Stockmayer, W. H. (1974) *J. Chem. Phys.* **60,** 12–21.
12. Bruns, W. (1977) *J. Phys. A Math. Gen.* **10,** 1963–1975.
13. Kranbuehl, D. E. & Verdier, P. H. (1977) *J. Chem. Phys.* **67,** 361–365.
14. Olaj, O. F., Lantschbauer, W. & Pelinka, K. H. (1980) *Macromolecules* **13,** 299–302.
15. Rudnick, J. & Gaspari, G. (1986) *J. Phys. A Math. Gen.* **19,** L191–L193.
16. Fougere, F. & Desbois, J. (1993) *J. Phys. A Math. Gen.* **26,** 7253–7262.
17. Fuller, G. G. (1995) *Optical Rheometry of Complex Fluids* (Oxford Univ. Press, New York).
18. Ferry, J. D. (1980) *Viscoelastic Properties of Polymers* (Wiley, New York).
19. Kornberg, A. & Baker, T. A. (1991) *DNA Replication* (Freeman, New York).
20. Wirtz, D. (1995) *Phys. Rev. Lett.* **74,** 2348–2351.
21. Leduc, P., Haber, C., Bao, G. & Wirtz, D. (1999) *Nature (London)* **399,** 564–566.
22. Yanagida, M., Hiraoka, Y. & Katsura, I. (1982) *Cold Spring Harbor Symp. Quant. Biol.* **47,** 177–192.
23. Haber, C. & Wirtz, D. (2000) *Biophys. J.* **78,** in press.
24. Baumann, C. G., Smith, S. B., Bloomfield, V. A. & Bustamante, C. (1997) *Proc. Natl. Acad. Sci. USA* **94,** 6185–6190.
25. Hagerman, P. J. (1988) *Annu. Rev. Biophys. Biophys. Chem.* **17,** 265–286.
26. Aronovitz, J. A. & Nelson, D. R. (1986) *J. Phys. (Orsay, Fr.)* **47,** 1445–1456.
27. Marko, J. F. & Siggia, E. D. (1995) *Macromolecules* **28,** 8759–8770.
28. Marko, J. F. & Siggia, E. D. (1995) *Phys. Rev. E Stat. Phys. Plasmas Fluids Relat. Interdiscip. Top.* **52,** 2912–2938.